EXPERIMENTAL AND NUMERICAL ANALYSIS OF CLT FLOOR SUBASSEMBLIES UNDER CATENARY ACTION

World Conference on Timber Engineering Oslo 2023

EXPERIMENTAL AND NUMERICAL ANALYSIS OF CLT FLOOR SUBASSEMBLIES UNDER CATENARY ACTION

Alicja C. Przystup[1], Thomas Tannert[2], Yong Lu[3], Thomas Reynolds[4]

ABSTRACT: Behaviour under combined axial tension and out-of-plane bending, typically observed in catenary action after loss of a support, was investigated on Cross Laminated Timber (CLT) floors. Uni-axial tension tests as well as combined tension and bending tests on CLT component and floor subassembly levels with screw butt joints and varying boundary conditions were performed. Bending moment capacity was shown to decrease with increasing of horizontal tension on the connection. Combined loading failure envelope was developed to observe a correlation between the test results of different scale, showing the potential of using component tests as predictors of the behaviour of more complex subassemblies.

KEYWORDS: Robustness, disproportionate collapse, progressive collapse, catenary action, combined loading

1 INTRODUCTION

1.1 Background

Robustness of large-scale mass timber buildings has become an important design consideration with their rise in scale and popularity [1]. The current tallest timber building is over 86m in height [2], and timber is increasingly widespread in multi-storey buildings. Ensuring that localised accidental damage will not result in disproportionate and progressive collapse is a vital design step that could save lives [3]. Eurocode robustness [4] design guidance is material independent. Since this objective-based approach is based on research conducted before mass timber was a commonly used construction material, research is required to provide design parameters and to ensure that the Eurocode framework can be reliably applied to mass timber. This need for more research and new comprehensive design guidance has been recognised by researchers and industry alike [5,6].

1.2 Catenary action in mass timber

One of the primary load resistance mechanisms after the loss of a load-bearing member is catenary action, which allows for redistribution of load in the structure [7] as visualised in Figure 1. It is also the main load redistribution mechanism allowed for in Eurocode 1 [4], which provides formulas for horizontal and vertical tie forces required for catenary to form. Under catenary action, the floors are subjected to combined bending and tension and therefore understanding of the effect of such combined loading on mass timber connections is instrumental for effective modelling and performance-based design. To date some early experimental work has been performed at a substructure level [8,9], but empirical data is lacking on the behaviour of variety of connections and types of engineered wood products used in practice.

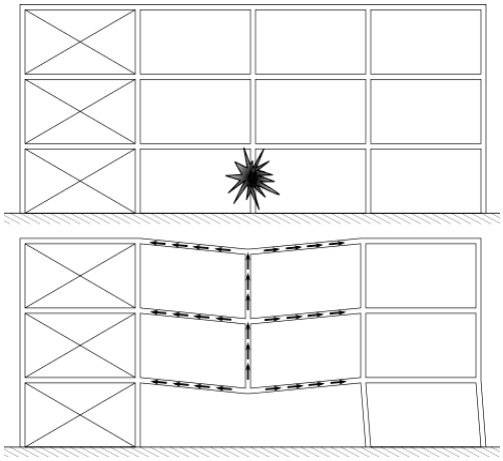

Figure 1: *Catenary action after compressive element loss*

1.3 Objective

The goal of the project presented in this paper was to apply a combined axial load and bending test method on substructures and components of mass timber floor systems that produces data to model the redistribution of forces in various substructure configurations. This correlation observed between the different scales of test results show that there is possibility for the component tests to be good predictors of the behaviour of the more complex subassemblies.

[1] Alicja Przystup, University of Edinburgh, Edinburgh, Scotland, a.c.przystup@sms.ed.ac.uk
[2] Thomas Tannert, University of Northern British Columbia, Prince George, BC, Canada, thomas.tannert@unbc.ca
[3] Yong Lu, University of Edinburgh, Edinburgh, Scotland, Yong.Lu@ed.ac.uk
[4] Thomas Reynolds, University of Edinburgh, Edinburgh, Scotland, T.Reynolds@ed.ac.uk

https://doi.org/10.52202/069179-0042

2 MATERIALS AND METHODS

2.1 Combined loading

The experiments were designed to investigate the influence of the applied tensile force on rotational stiffness, ultimate strength, and maximum angle of rotation of the floor panel-to-panel connection. A test method adequate for this purpose is one that can be replicated for multiple types of connections; therefore, it ought to be easily repeatable and cost effective. Since full-span set-ups might not be necessary to isolate the connection behaviour, a component test was proposed alongside full-span floor tests to investigate influence of specimen size. The free body diagram shown in Figure 2 allowed for conversion of the pushdown force P, applied tension at supports T, and displacement u data into moment M (Equation 1) and rotation θ. This allowed for direct comparison of the connection behaviour independently of scale.

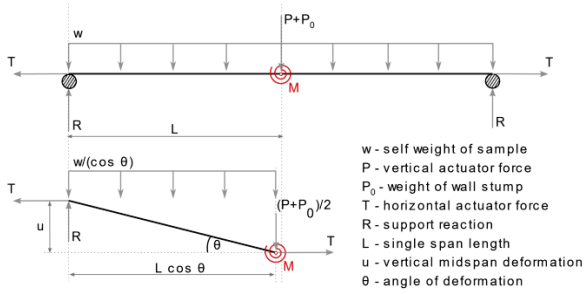

Figure 2 *Free body diagram of the tests*

$$M = \frac{P \cdot L\cos\theta}{2} + \frac{P_0 \cdot L\cos\theta}{2} + \frac{\omega \cdot L^2 \cos\theta}{2} - T \cdot u \qquad (1)$$

This calculated bending moment resistance of the connection in case of a butt joint will come from the moment couple forming between the compressive force forming at the top face and tension in the screws (Figure 3), which can be calculated as per Equation 2.

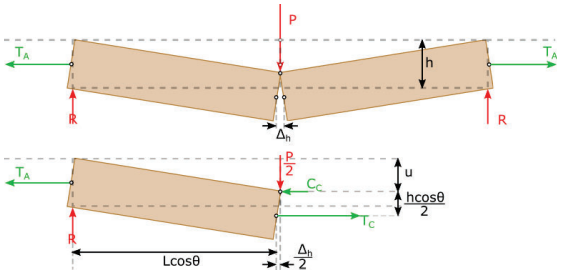

Figure 3: *Free body diagram showing the resultant connection forces dependant on component geometry*

$$T_c = P \cdot \frac{L}{h} + T_A \cdot \left(1 - \frac{2u}{h}\right) \qquad (2)$$

2.2 Materials

The CLT panels used were 5-ply 100 mm thick Binderholz BBS 125 of 20-20-20-20-20 mm layer thickness and 10% moisture content. SWG fully threaded self-tapping screws (STS) ϕ8 mm x 140 mm installed at 45° angle were used to make a butt connection, as shown in Figure 4. The full-scale test specimens had a width d = 600 mm and either 4 or 6 screws with spacings of a = 130 mm, b = 260 mm and c = 110 mm; the tension as well as component specimens had the width of d = 400 mm and spacings a = 110 mm, b = 100 mm and c = 90 mm.

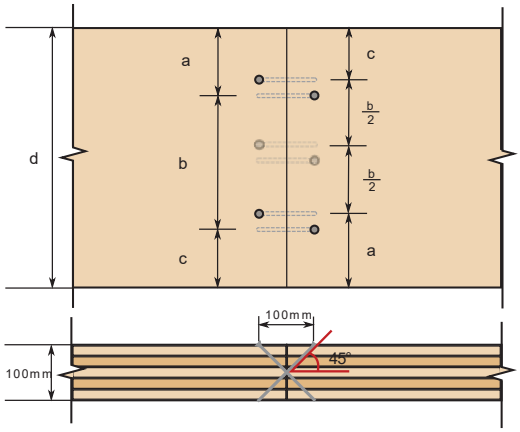

Figure 4: *Butt-joint connection design*

2.3 Axial tension tests

The horizontal force and stiffness of the connection is instrumental in dictating the force-displacement behaviour, the ultimate strength and deformation of the catenary substructure. It is therefore necessary to measure the mechanical behaviour of the connection under pure axial loading. To eliminate any bending effects of gravity loading, an upright configuration was chosen (Figure 5). The samples were attached with 6 tight-fit 15 mm diameter steel dowels on each side to minimise the slack in the system. Displacement was measured by two potentiometers installed on either side of the connection. The connections design was the same as in the component tests and therefore tension test results were also used as the equivalent of the combined test loads under maximum utilisation of tension (100% T).

Figure 5 *Axial tension test experimental setup*

https://doi.org/10.52202/069179-0042

2.4 Component tests

The component tests (Figure 6) were performed on the same test set-up as the full-span tests (Figure 7), but with the wall supports moved inwards to create the desired shorter span. The aim of the component tests was to gather information on the influence of tension level on the moment rotation behaviour and ultimate limit state values; therefore, the test series were designed in even increments of tension utilisation from 0%-75% (Table 2). These utilisation ratios were based on the average ultimate strength obtained from the axial tension tests. Together with the axial tension tests this allows for investigating of the changes in mechanical bending properties depending on the tensile utilisation ratio.

Figure 6: *Component test experimental setup*

Table 1: *Connection utilisation ratios in component tests*

Series	Tension utilisation	Tension (kN)	#STS
C1-B-0	0%	0.00	4
C1-B-25	25%	7.96	4
C1-B-50	50%	15.91	4
C1-B-75	75%	23.87	4

2.5 Full-span tests

The full-span pushdown tests were performed in 3-point bending on two butt-jointed panels with an effective length (midspan to support) of 3000 mm, see Figure 6. Four vertical string pots on either side were placed at 1 m increments and two additional string pots at the underside of the connection to monitor the joint opening.

The first full-span floor specimens were tested in a simply supported arrangement. This was used to verify whether moment rotation behaviour of the connection remained the same in such larger subassemblies as the component tests. Later specimens were tested using a variety of wall details and support conditions.

The problem with comparing tests of different spans while section size and connection design remain unchanged is the increase in relevance of the compressive arching, as it is directly proportional to the section depth to span ratio. To mitigate that issue, the tension was applied utilising chains rather than fixing the support to another member or directly to the strong wall, while the sample rested above steel rollers. That way, there was no horizontal compressive reaction possible aside from friction from the rollers which can be assumed to be negligible. Therefore, in this setup compressive arching was largely eliminated. The load was applied by two actuators, one vertically at midspan for pushdown and one installed horizontally on one end of the assembly for axial load application.

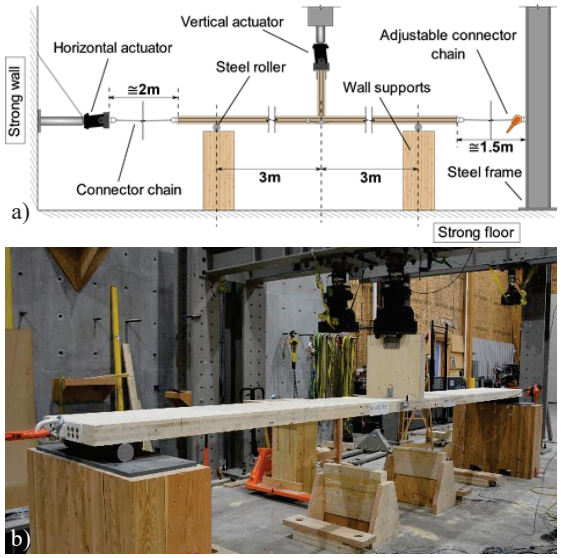

Figure 7 *Full-span test setup: a) schematic, b) photo*

Five variables were changed across the test series, summarised in Table 2. The first is the point of load application through the wall stump which either done by placing the wall loosely on top (*loose)* or attaching the load with one pair of Simpson ABR105 CLT angle bracket angle brackets installed on both sides close to the centre (*anchored)*. The second parameter was the support condition which was either simple *pin* or simulated double continuous span behaviour through restraining the overhang (*restrained)*. The tests had either 6, 4 or no screws (*#STS*). The series with no screws relied solely on the angle brackets (S5-N-P-L-15) and was performed as a control of the remainder of the tests using that connection alongside the butt joint.

Table 2: *Test series overview in full-span tests*

Series	Load	Support	T (kN)	STS
S1-B-P-L-15	Loose	Pin	15	6
S1-B2-P-L-15	Loose	Pin	15	4
S2-B-P-L-30	Loose	Pin	30	6
S2-B2-P-L-30	Loose	Pin	30	4
S3-B-P-A-15	Anchored	Pin	15	4
S4-B-P-A-F	Anchored	Pin	Fixed	4
S5-N-P-L-15	Anchored	Pin	15	0
S6-B-P-L-F	Loose	Pin	Fixed	4
S7-B-R-L-30	Loose	Restrained	15	4

https://doi.org/10.52202/069179-0042

3 RESULTS AND DISCUSSION

3.1 Axial tension tests

The axial tension test results are shown in Figure 8. An initial high-stiffness elastic region is followed by a peak and a softening branch. The mean value of the maximum force is 31.8 kN from the four tests. After around 6 mm displacement, the load reached a plateau, in most cases, at approximately 15 kN, until failure.

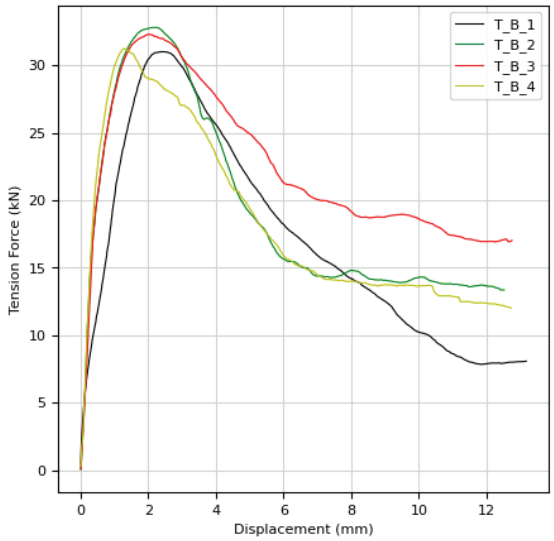

Figure 8: *Axial force displacement curves*

The initial stiffness k_0, maximum tension force T_{max}, and its corresponding deformation U_{Tmax} as well as the deformation at 50% load drop-off U_{T50} are summarised in Table 3. The latter is presented to investigate the extreme deformation behaviour which was relatively plastic. The long plateau of plastic behaviour after the initial drop-off past peak value could potentially allow for sufficient deformation to decrease tensile demand. However, the rapid loss of stiffness would lead to accelerations in the system and further release of kinetic energy. This would likely negate the initial benefits from this type of deformation and still result in connection failure.

Table 3 *Axial force test results summary*

Specimen	k_0 (kN/mm)	T_{max} (kN)	U_{Tmax} (mm)	U_{T50} (mm)
T-B-1	8.367	31.00	4.67	10.80
T-B-2	9.290	32.80	4.78	9.27
T-B-3	9.195	32.28	4.55	18.33
T-B-4	9.138	31.22	3.85	9.98
mean	8.998	31.83	4.46	12.09
CoV	4%	2%	9%	34%

3.2 Component tests

The maximum force, displacement, moment and rotation of the component-level tests are summarized in Table 4. In Figure 9, the force displacement behaviour of one specimen from each series is plotted to illustrate the main variabilities. The maximum vertical force resistance as well as maximum rotation initially increase between series C1-B-0 and C1-B-25, with one of the latter samples not failing fully after reaching the maximum actuator stroke (Figure 11a). This demonstrates activation of the catenary action. The benefit of the tensile force to the overall strength in comparison to the bending only series is also clearly visible in the C1-B-50, however with a relatively lower deformation capacity from C-B-25. The last test series with 75% tension utilisation ratio had vertical force resistance comparable to the bending only samples, but with a much higher variability.

Table 4: *Component test results summary*

Series	P_{max} (kN)	U_{max} (mm)	M_{max} (kNmm)	θ_{max} (rad)	Fracture (y/n)
C1-B-0	4.10	55.2	1668	0.028	y
	4.10	62.3	1668	0.026	y
	4.03	95.2	1640	0.028	y
	3.58	249.6	1461	0.026	y
C1-B-25	10.90	476.0	1779	0.442	n
	5.91	241.4	1336	0.035	y
	3.71	133.7	1349	0.036	y
	6.29	253.1	1278	0.035	y
C1-B-50	4.39	84.9	910	0.049	y
	4.24	91.1	894	0.042	y
	7.57	155.3	1068	0.188	y
	3.77	73.3	898	0.035	y
C1-B-75	5.78	65.8	1101	0.055	y
	0.11	16.0	71	0.003	y
	3.96	76.2	692	0.056	y
	5.41	270.7	960	0.074	y

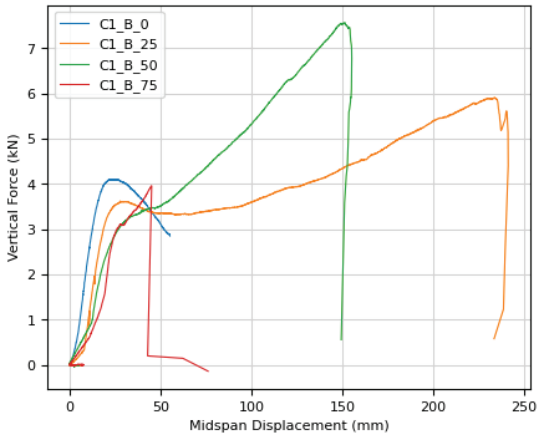

Figure 9: *Component test force displacement curves*

The maximum moment capacity of the connection, which can be observed as the peak values in Figure 10, drops proportionally to the level of tension applied to the connection. It can also be observed that the specimens loaded to the middle range of force between 25-50% performed best both in maximum deformation and

maximum force. However, all the tests reached their maximum moment at the same rotation of approximately 0.04 rad. Any further increase in vertical force resistance for the C1-B-25 and C1-B-50 samples occur directly from catenary action activation, which is only possible through the post-failure plastic plateau.

Failure of the screws in the component tests was observed in two different modes. Screws failed in withdrawal, with some having punched through the material from the headed side of the screw (Figure 11b). In either scenario material in the traverse layers of the panels was pulled due to the tension perpendicular to the grain. Some of that failure was shown to split all the way to the edge of the sample, indicating that a higher edge spacing and therefore more material to distribute the localised stresses could have a positive impact on the overall strength of that connection.

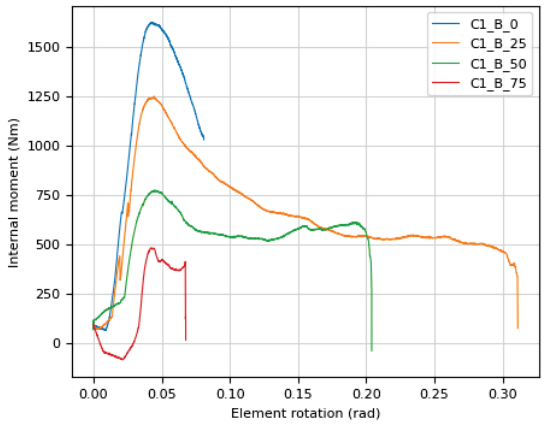

Figure 10: *Component test moment rotation curves*

Figure 11: *Butt joint component tested to maximum stroke (a) and to failure (b)*

3.3 Full span tests

Maximum force, displacement, moment, and rotation values recorded for each test are summarized in Table 5. One of the challenges of full-span testing was the relatively low vertical stroke to span ratio, which led to some of the samples not failing throughout the duration of the test (greyed out fields), meaning that their maximum values will likely be larger than the tabulated data shown.

Table 5: *Full span test results summary*

Series	P_{max} (kN)	U_{max} (mm)	M_{max} (kNmm)	θ_{max} (rad)	Fracture (y/n)
S1-B-P-L-15	5.53	498.1	2120	0.167	n
	5.81	487.9	2739	0.163	n
	5.57	434.2	2059	0.145	y
	5.68	522.3	2031	0.175	n
S1-B2-P-L-15	5.30	497.7	1814	0.167	n
	2.29	262.7	1284	0.088	y
	2.44	287.1	1233	0.096	y
	2.07	252.6	1233	0.084	y
	3.36	338.8	1438	0.113	y
	5.17	499.8	1563	0.167	n
S2-B-P-L-30	3.05	144.7	1757	0.048	y
	2.46	128.7	1348	0.043	y
	8.31	401.7	1794	0.134	y
	4.26	230.1	1303	0.077	y
S2-B2-P-L-30	1.90	117.8	1227	0.039	y
	0.02	45.6	1307	0.015	y
	2.06	121.7	1287	0.041	y
	0.43	65.5	1227	0.022	y
S3-B-P-A-15	5.12	437.9	2464	0.146	y
	4.25	375.2	2438	0.125	y
	5.20	454.9	2587	0.152	y
	5.34	495.8	2765	0.166	y
S4-B-P-A-F	3.39	489.6	1186	0.164	n
	3.72	486.4	1149	0.163	n
	3.68	449.4	1260	0.150	y
	2.99	391.3	1273	0.131	y
S5-N-P-L-15	0.54	2.5	2243	0.001	y
	0.55	101.0	1433	0.034	y
	0.24	31.9	1705	0.011	y
S6-B-P-L-F	2.86	230.2	1248	0.077	y
	2.26	264.6	1160	0.088	y
	1.96	227.6	1242	0.076	y
	1.73	215.6	1196	0.072	y
S7-B-R-L-15	16.49	155.9	1144	0.052	y
	15.25	140.3	879	0.047	y
	14.09	127.6	690	0.043	y
	18.31	162.2	1239	0.054	y

The shape of the load displacement curve is strongly influenced by the way in which the axial tension is applied, which confirms that the catenary action is the primary load resistance mechanism. For instance, in the test series where tension was increasing along with pushdown through fixed horizontal displacement (S4 and S6), the support stiffness of the system increased

https://doi.org/10.52202/069179-0042

throughout the test (Figure 12). The maximum tension values at supports for these test series are shown in **Error! Not a valid bookmark self-reference.**. The presence of angle brackets connecting the wall stub to the floor panels did not have a great influence on the maximum tension capacity; however, it did allow for a greater deformation which positively affects the overall force capacity presented in Figure 12.

Table 6: *Maximum tension in the fixed horizontal displacement tests*

	T_{max}	U_{Tmax}
S6-B-P-L-F	19.5	152.9
	16.5	120.6
	16.3	155.9
	15.2	113.8
mean	**16.9**	**135.8**
CoV	11%	16%
S4-B-P-A-F	14.0	243.5
	19.4	227.8
	15.0	167.6
	15.7	185.6
mean	**16.0**	**206.1**
CoV	15%	17%

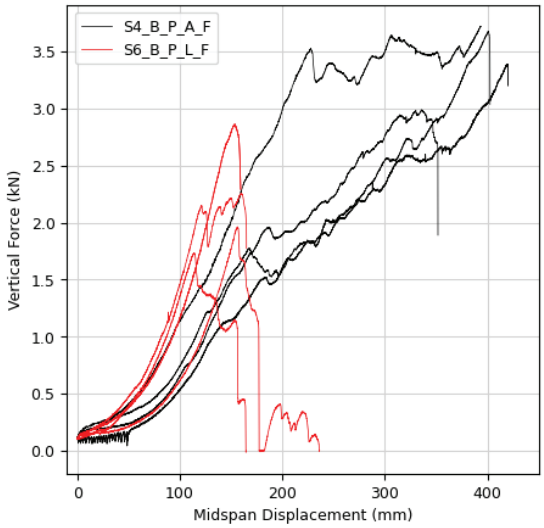

Figure 12: *Fixed displacement tests force displacement curves*

The effect of the additional brackets in samples S3-B-P-A in the load hold is less apparent, showing almost exactly the same behaviour as their S1 counterparts under the same 15 kN loading, see Figure 13. This is because due to the load control nature of the loading even a small drop-off in tensile force will lead to the actuator rapidly increasing the rate of displacement and therefore causing immediate failure. The caveat of such tests is if the connection does in fact have some remaining strength after that initial peak, but reduced stiffness, this will allow for greater deformation and therefore decreased tension demand, allowing to potentially achieve load equilibrium once again. However, the majority of timber connections being relatively brittle do not in fact have a large enough residual strength to be able to accommodate the resulting kinetic effect. Moreover, with the large variability of timber, especially in the region close to failure, it would not be safe to rely on this behaviour past the peak strength as a robustness design feature.

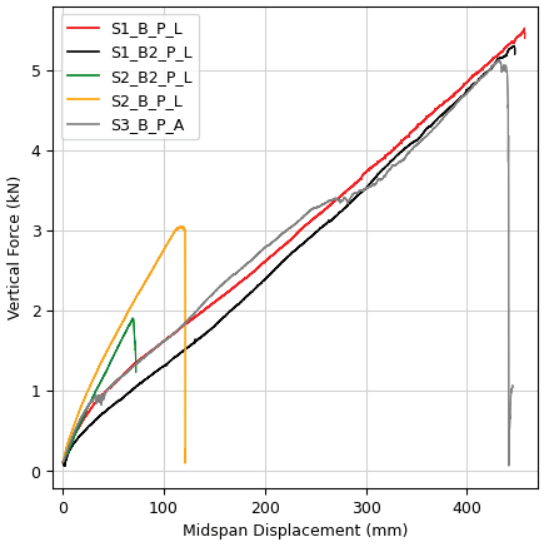

Figure 13: *Selected axial load hold tests force displacement curves*

Results of the test series which were tested over roller supports and in the horizontal tension load hold are presented in Figure 14. The stiffness of the system is again largely governed here by the tension and therefore the test series S2_B and S2_B2 which are under 30 kN horizontal load hold are visibly stiffer in comparison to the S1_B, S1_B2 and S3_B which were loaded with 15 kN. Notably, the number of screws (S1_B and S2_B with 6 screws total and S1_B2 and S2_B2 with 4 screws total) nor the presence of the wall bracket connection did not visibly affect the stiffness. Both the wall brackets and the extra pair of screw did have a positive effect on the ultimate load and moment capacity and maximum deformation/rotation as seen in Table 5.

The samples that have been tested to full failure, just as in the component tests, were observed to have failed in screw withdrawal, see Figure 14a. Most of them did not however have the layer split travel to the edge of the sample, which could be due to the extra 20 mm edge spacing. Connections in both full-scale and component tests were designed well within the minimum spacing, therefore when designing for large deformations, the guidance made for connections for the elastic limit might not apply in the same way.

Samples with the continuous span have produced the highest vertical force resistance of 14-18 kN, with more than 3x higher resistance than the catenary action. The failure mode of these samples was initially rolling shear in the traverse layers and eventually tensile splitting of the uppermost layer (Figure 14b). The test was stopped after this first load drop off due to the panel failure and before the ultimate failure of the connection due to safety concerns. The maximum moment exhibited by the

connection was on average lower than but approaching the values in series S1-B2 of the equivalent connection properties and magnitude of tension applied. This explains lack of connection failure but also implies that it was imminent, and the overall force capacity of the system was unlikely to rise back up above the initial peak.

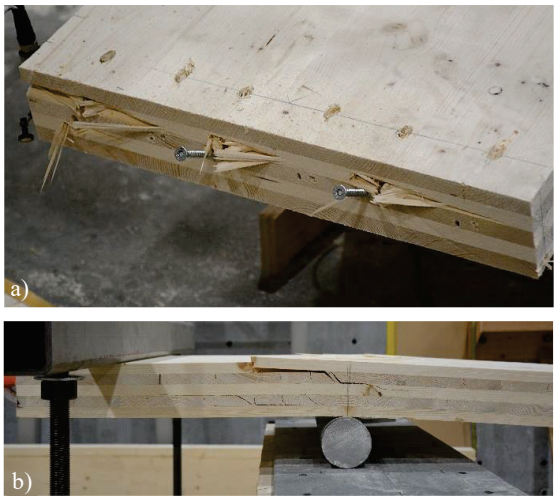

Figure 14: *Failure of the connection in test series S1 (a) and over the support in test series S6 (b)*

3.4 Combined analysis

Internal connection tension forces in selected component tests derived from equilibrium of forces as per Eq.2 are shown in Figure 15. In essence the tension present in the connection is a combination of the moment couple present from the opening of the joint and the tension resultant from catenary forces.

Although this was similarly visible in the component tests, several differences can be observed between tension displacement behaviour when comparing to the uniaxially loaded specimen illustrated in Figure 9. This was due to the slight changes in the failure modes, as the bent screws redistributed internal loads differently based on the angle of deformation. The ultimate strength however remained consistent across all samples, which means that despite different bi-axial load combinations this can be the reliable parameter for failure checks.

Results of the pin-support tests under constant tension have been summarised as a failure envelope for combined tension and bending in Figure 16. Each datapoint represents the maximum moment experienced by the sample and the corresponding tension utilisation value based on the axial load tests. An extreme value distribution analysis was performed on the results from 4 specimen in each of the component test series and linear regression lines were fitted through the corresponding median values and the upper and lower bounds of the 95% confidence interval.

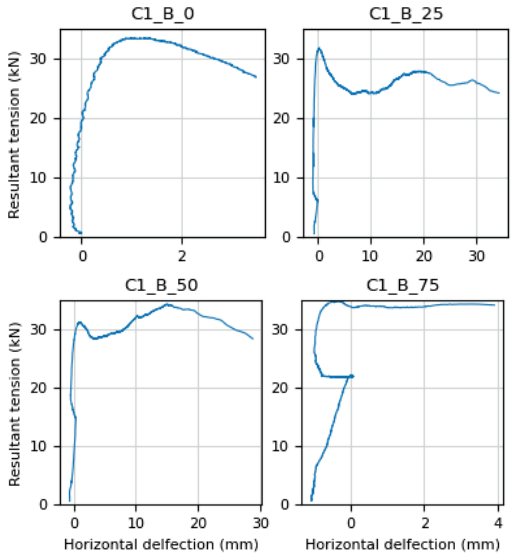

Figure 15: *Internal tension forces in component test results*

The moment capacity of both component and full span tests drops proportionally to the increased tensile utilisation. Horizontal withdrawal of the screw is the governing failure mode and both increased system tension as well as bending of the connection increase the tension resultant at the screw, therefore this relationship is numerically justified. As shown in Figure 15, the total of those two resultants reaching tensile capacity of the connection is the cause of connection failure.

The values of the full-span tests when compared to the component test data fit does fall on the higher side of the data distribution. This could be due to a multitude of factors such as data errors and the active changes in the effective span due to the horizontal travel distance of steel rollers, small changes in screw spacing and proportionally large variability of timber properties. However, they do still largely follow the same trend and are a deemed a good predictor of the large-scale behaviours.

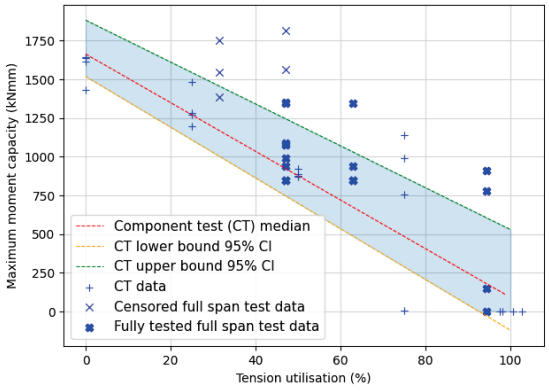

Figure 16: *Combined loading failure envelope*

https://doi.org/10.52202/069179-0042

4 CONCLUSIONS

The presented tests provide much-needed insight into the possibilities of smaller scale experiments as a base for empirical-based robustness analysis of mass timber floor systems. This correlation observed between the different scales of test results show that there is possibility for the component tests to be good predictors of the behaviour of the more complex subassemblies.

The analysis has shown that the tension increase in the system has both beneficial and compromising effects on the total force capacity on the system – the tension allows for the load redistribution to form, consequently lessening the bending capacity demand on the system, but at the same time decreases the bending capacity itself. In the tested samples the region where these two were balanced was between 25-50% of tension utilisation. However, the maximum moment capacity is consistently being reached at minimal deformations and the subsequent catenary activation occurs on a sample effectively past its failure load. Moreover, the variability of results increases drastically at the higher end of the utilisation scale meaning that relying on that behaviour is not advised.

The paper presents testing that can form the basis of future performance-based design frameworks. Still, a significant amount of research is needed to develop comprehensive, functional design guidance. Aiming for standardisation of test, modelling and design methods is essential for continuous growth of the industry and use of timber as modern construction material for years to come.

ACKNOWLEDGEMENTS

The authors acknowledge the financial support received by the Royal Society of Edinburgh Lessels Travel Scholarship. The experimental work was funded by the government of Canada through a Canada Research Chair. The support by the UNBC technicians Michael Billups, James Andal, and Ryan Stern is greatly appreciated.

REFERENCES

[1] Mpidi Bita H, Tannert T. Tie-force procedure for disproportionate collapse prevention of CLT platform-type construction. *Engineering Structures* 189(2):195–205, 2019.

[2] Abrahamsen R. Mjøstårnet: Construction of an 81 m tall timber building. 23. In: Internationales Holzbau-Forum IHF 2017, 1–13. 2017.

[3] Starossek U, Haberland M. Robustness of structures. *Int J Lifecycle Performance Engineering*. 1(1):3–21. 2012.

[4] European Committee for Standardization. Eurocode 1 - Actions on structures - Part 1-7: General actions - Accidental actions BS EN 1991-1-7:2006.

[5] COST Association AISBL. Memorandum of Understanding for the implementation of the COST Action “Holistic design of taller timber buildings” (HELEN) CA20139. Brussels; 2021.

[6] Voulpiotis K, Köhler J, Jockwer R, Frangi A. A holistic framework for designing for structural robustness in tall timber buildings. *Engineering Structures*. 227:111432, 2021.

[7] Kiakojouri F, de Biagi V, Chiaia B, Sheidaii MR. Progressive collapse of framed building structures: Current knowledge and future prospects. *Engineering Structures.* 206:110061, 2020.

[8] Mpidi Bita H, Tannert T. Experimental Study of Disproportionate Collapse Prevention Mechanisms for Mass-Timber Floor Systems. *ASCE Journal of Structural Engineering.* 146(2):04019199, 2020.

[9] Lyu CH, Gilbert BP, Guan H, Underhill ID, Gunalan S, Karampour H, et al. Experimental collapse response of post-and-beam mass timber frames under a quasi-static column removal scenario. *Engineering Structures* 213:110562, 2020.